Experimental Thermal and Fluid Science 95 (2018) 88–95

Contents lists available at ScienceDirect

Experimental Thermal and Fluid Science

journal homepage: www.elsevier.com/locate/etfs

Spontaneous ignition of wildland fuel by idealized firebrands

N. Hernández[a], A. Fuentes[a,*], J.L. Consalvi[b], J.C. Elicer-Cortés[c]

[a] Departamento de Industrias, Universidad Técnica Federico Santa María, Av. España 1680, Casilla 110-V, Valparaíso, Chile
[b] Aix-Marseille Université, IUSTI/UMR CNRS 7343, 5 rue E. Fermi, 13453 Marseille Cedex 13, France
[c] Universidad de Chile, Departamento de Ingeniería Mecánica, Beauchef 850, Piso 5, Santiago, Chile

ARTICLE INFO

Keywords:
Ignition time
Wildland fuel
Critical heat flux
Firebrand
Wildfire

ABSTRACT

The spontaneous ignition of a forest fuel layer by idealized firebrands was carried out experimentally in a bench scale apparatus designed to understand the relationship between the time to ignition and incident radiative heat flux on a ring-shaped forest fuel litter. Time to ignition, mass loss, radial temperatures and incident radiative heat flux were measured. The fuel samples were Radiata Pine needles, representative of Chilean forests and the influence of the physical characteristics of the fuel load were analyzed. The firebrand was idealized using a cylindrical electric heater capable of releasing heat flux up to 26.7 kW/m^2. For the fuel beds considered the inverse of ignition time was found to be linearly dependent on the incident radiative heat flux, typically observed for thermally thin solid fuels. Several tests were carried out in order to estimate the critical (minimum) heat flux for spontaneous ignition for two forest fuel loads. Additionally, a quasi-linear relationship between mass loss rate and incident radiative heat flux was experimentally determined.

1. Introduction

The wildland-urban interface (WUI) is the zone where housing structures meet or interact with wildland vegetation. WUI fires occur when wildland fires cannot be controlled, often due to extreme wind and fuel conditions, and spread into communities. These fires have been a large problem over the last years not only in Chile [1], but also all over the world. The most recent event took place during year 2017, a wildfire described as the worst in the modern Chilean history, with a peak of 142 simultaneous fires foci being probably generated by fire spotting processes, destroying over 5000 km^2 and 1000 buildings.

If a wildfire involves the production of flaming or glowing particles (firebrands) transported by the convective plume, which may cause new secondary fires ahead of the main front, the ignition mechanism is called spotting [2]. The spotting mechanism can be described in three main sub-processes: (i) the generation of firebrands from vegetation and structures, (ii) subsequent transport normally through the convective plume and by the wind [3] and (iii) the ignition of the forest fuel at landing position [4]. Nowadays a main challenge is understanding how these firebrands can ignite, create new fire foci over a forest fuel layer [2] and how it spreads. Many modelling attempts have been carried out in order to predict the fire spread including the mathematical complexity of the stochastic spotting process [5], however this issue has not been fully solved yet.

The transport of firebrands and associated models have been widely discussed in the literature [6–9]. Nevertheless, very few publications have addressed the issues of ignition due to firebrands and ignitability of fuel beds. Blackmarr [10] and Ferreira [11] carried out experiments with point-source ignitions using dropped lit matches. Manzello et al. [12,13] developed some experiments using a bench scale apparatus to produce firebrands which were deposited on common fuel litters of WUI. Ellis [14] tested the probability of ignitability of pine needles using flaming and glowing brands made of eucalyptus and the moisture content of the fuel bed was varied. Some authors have investigated the ignition considering only the characteristics of the fuel litter [10,11,15]. Ganteaume et al. [16] have carried out experiments including the characteristics of fuel beds and firebrands. Recently numerical models were developed to evaluate basically the probability to ignite or generate new fires using theoretical firebrands [3,17]. This work can be also complemented by Manzello et al. [18] where the size and mass distributions of firebrands from pine trees were established.

In fires, piloted ignition takes place with the presence of an ignition source such as a spark or a flame as opposed to spontaneous ignition which occurs without any ignition source. White et al. [19] conducted tests of piloted ignition at fixed heat flux of 25 kW/m^2 in a cone calorimeter on branches from various coniferous trees, studying the dependency of ignition time on moisture content. Dimitrakopulos and Papaioannou [20] tested the piloted ignitability of vegetation at fixed flux of 45 kW/m^2, where the main goal was to determine the moisture content necessary so that no ignition would occur during 300 s of

* Corresponding author.
E-mail address: andres.fuentes@usm.cl (A. Fuentes).

https://doi.org/10.1016/j.expthermflusci.2018.01.037
Received 30 January 2018; Received in revised form 30 January 2018; Accepted 31 January 2018
Available online 02 February 2018
0894-1777/

Nomenclature

A	area (m^2)
h	height (m)
I	current intensity (C)
m	mass (kg)
L	length (m)
l	thickness (m)
q	heat (J)
r	radius (m)
t	time (s)
T	temperature (K)
TC_j	temperature at position j (K)
u	uncertainty (–)
v	volume (m^3)
V	voltage (V)

Greek symbols

α	volume fraction (–)
ϵ	porosity (–)
η	mass loss (–)
ρ	density (kg/m^3)
σ	Stefan-Boltzmman constant ($W/m^2\,K^4$)
ω	surface to volume ratio (m^{-1})

Subscripts

0	initial
b	bulk
bb	blackbody
cri	critical
elec	electrical
emit	emitted
fuel	fuel (pine needles)
h	heater element
i	inner
ig	ignition
inc	incident
o	outter

Superscripts

$()''$	per unit area
$(\cdot)$	per unit time

exposure period. Piloted ignition was also carried out by Mindykowsky et al. [21] testing pine needles and kermes oak leaves varying the bulk densities and the imposed external heat flux up to 30 kW/m^2, the time to ignition and critical heat flux were studied and a thermal model was analytically derived from thermally thin assumption.

On the other hand, some researchers have performed autoignition experiments by radiant ignition, using only an external heat flux. Filippov [22] measured the radiant heat flux needed for autoignition on many different types of forest materials, but moisture content was not specified and time to ignition was measured and correlated to irradiance. Trabaudd [23] exposed a variety of vegetation types at a fixed flux of 25 kW/m^2 and measured the autoignition time as a function of moisture content. Tihay et al. [24] have measured the influence of diameter of dead shrub twigs on autoignition experiments, time to ignition, surface temperature and mass loss, among others were analyzed. Recently in the works of Urban et al. [25] idealized hot elements (geometry and temperature) were used to understand the ignition in a controlled fuel bed.

Unfortunately, as indicated above only few studies have been performed in piloted or spontaneous ignition where the geometries of firebrand are completely controlled. Furthermore, to the best knowledge of the authors, experiments of spontaneous ignition by idealized firebrands under controlled radiative heat flux including variations on the physical characteristics of the fuel litter have not been addressed. In this sense, an experimental bench scale apparatus has been designed and implemented to study the spontaneous time to ignition of idealized

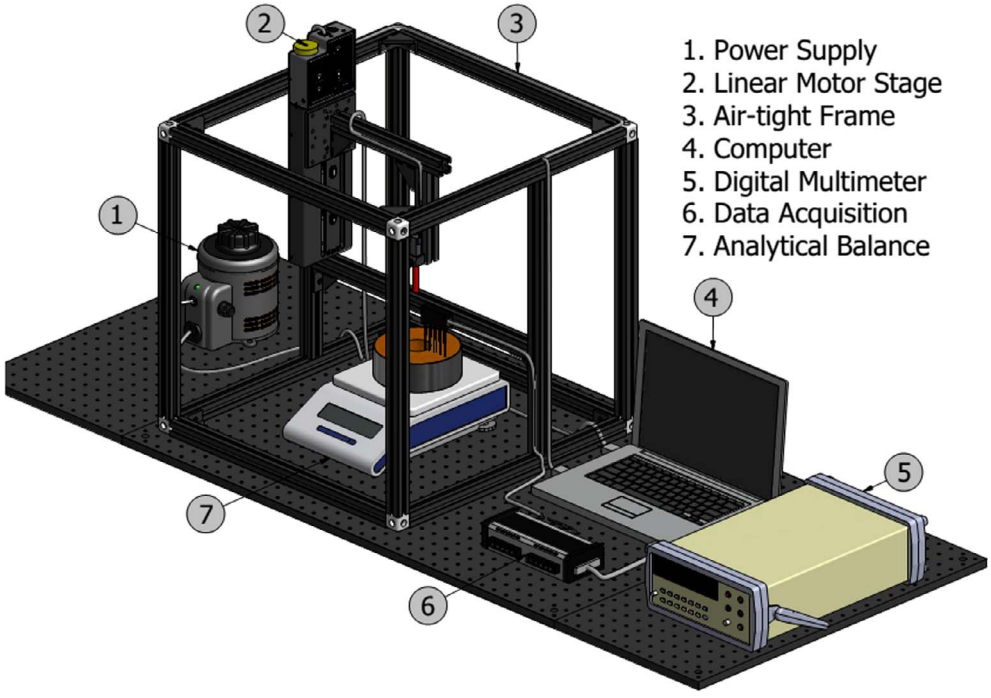

Fig. 1. Schematic of the experimental set-up.

firebrands in a common forest fuel layer. The apparatus allows to measure time to ignition for different fuel litters. The mass loss fuel and the radial temperatures inside the forest fuel layer were evaluated simultaneously at different radiative heat fluxes. The firebrand was idealized by means of an electric element heater and the forest fuel litter was Radiata Pine needles at two different bulk densities.

2. Experimental methodology

2.1. Bench scale apparatus

Spontaneous ignition experiments of pine needle litters were carried out in a bench scale apparatus described in Fig. 1. This device was designed and implemented to reproduce equivalent conditions of a single firebrand igniting a controlled forest fuel layer. As shown in the schematic of Fig. 1 the main experimental part consists of a volume protected with Plexiglas in order to avoid any interferences from the environment during the experiments, specially unwanted effects on the balance and the heater element. The firebrand in this case was idealized by an electric heater. This heater consists of a cylindrical-shaped element manufactured by Bach RC. The size of this element, comprised in the range of common firebrands [18], built in silicon nitride, is r_h=5 mm and the hot zone length is h=46 mm (see Fig. 2). This radiant heater has an emissivity between 0.7 and 0.8, an electrical resistance of 132 Ω and an operating range of up to 260 V. The heater was adequately positioned inside the forest fuel layer using a linear motor stage of 150 mm allowing small displacement steps of 0.1 μm. In order to measure the mass loss during the pyrolysis processes a Shimadzu high precision analytical balance model AUW-320 was implemented in the set-up, detecting small mass changes of 0.1 mg. The data recorded by the scale were treated by a data acquisition module IOtech Personal Daq 56 Series and then stored in the computer.

The specimen holder was simply a ring-shaped stainless steel basket open top. The basket has the following size r_o=130 mm and h=46 mm. A free path of r_i=20 mm (see Fig. 2) was kept free in order to place the electric heater. In the ring-shaped space the pine needles were randomly placed (see Section 2.3 *Distribution of Fuel Layer* for details). The temperature evolution inside the forest fuel litters was measured by five thermocouples type K regularly spaced, ranged along the radial axis and connected with the data acquisition system. The electric heater power supply was varied by using a variable transformer system reaching output voltages from 0 V up to 380 V. A Keithley 2100 Series digital multimeter was connected in parallel to measure the voltage during each experiment. The maximum voltage tested in the experimental campaign was 250 V.

2.2. Sample preparation

This study concerns dead and dried pine needles collected from Valparaiso region, Chile, namely Radita Pine (Pinus Radiata). In order to reduce the moisture content, the pine needles were oven-dried at 333 K at least 12 h, according to the procedure performed by Mindykowsky et al. [21]. After 12 h no further changes in mass measurements were observed, suggesting that no more moisture content remained in the fuel samples. Anyway, a weakly percentage of free moisture was found in the samples, coming from the self rehydration process.

2.3. Distribution of fuel layer

Initially a specific mesh was built and placed in the free path inside the basket in order to reduce the number of failed experiments. This occurred eventually by contact between the needles and the heater element surface during the pyrolysis process before the ignition. Therefore the forest fuel layer was placed in annular ring section (see Fig. 2).

The pine needles, selected one by one removing small debris, were randomly placed inside the basket and filling up from the bottom holder. Pine needles longer than the size of the holder were cut with scissors. The sample holder was filled with initial masses (m_0) of 18.5 g and 29.5 g of forest fuel. It is important to note that the volume of the sample was kept constant (holder volume) obtaining bulk densities ($\rho_b = m_0/v_{basket}$) ranging from 30.8 kg/m^3 to 49.2 kg/m^3.

2.3.1. Mass density

The procedure described by Tihay et al. [26] was followed in this experiment to determine the average mass density of pine needles. The methodology considers three steps: (i) A mass of fuel (m_{fuel}) was weighed and put into a graduated tube, (ii) 10 ml of isopropyl alcohol (v_{iso}) was added and finally (iii) the total volume (v_{total}) was measured. Tihay et al. [26] used ethanol instead of isopropyl alcohol, but there are no differences in the results. For this study 12 tests were carried out and the density of the sample was obtained from Eq. (1). The mean mass density was 615.5 ± 19.8 kg/m^3.

$$\rho_{fuel} = \frac{m_{fuel}}{v_{total} - v_{iso}} \tag{1}$$

2.3.2. Surface to volume ratio

This ratio was determined presuming that pine needles were cylindrical-shaped and only depends on the length (L) and thickness (l) as indicated in Eq. (2). A sample of pine needles was treated by image processing obtaining an average value of ω=2579.8 ± 58.7 m^{-1}.

$$\omega = \frac{2}{L} + \frac{4}{l} \tag{2}$$

Other parameters as porosity ($\epsilon = 1 - \rho_b/\rho_{fuel}$) and volume fraction ($\alpha = m_0/\rho_{fuel} v_{basket}$) are included and summarized in the following Table 1.

2.4. Heater characterization

2.4.1. Surface temperature

The first step in the characterization of the heater element (idealized firebrand) was to evaluate the surface temperature. The measurements were achieved with a thermocouple type K and the temperature was modified varying the voltage supplied to heater element. As expected, the surface temperature was symmetrical along the heater and the set of experiments followed the same trend as presented in Fig. 3a.

The maximum peak of temperature on the surface of the heater was obtained for 250 V reaching about 1150 °C and the minimum measured peak was 800 °C at 160 V. The largest difference observed between both

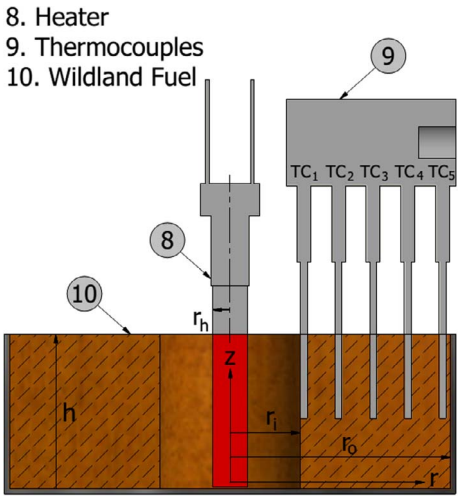

Fig. 2. Heater and thermocouples layout inside of forest fuel layer.

Table 1
Characterization of the forest fuel employed.

	m_0 (g)	ρ_b (kg/m^3)	α (–)	ω (m^{-1})	ϵ (–)
WF1	18.5	30.8	0.05	2579	0.95
WF2	29.5	49.2	0.08		0.92

ends of the heater was only 300 °C. The mean temperature was used in order to validate and to characterize the radiation released by the heater and particularly the incident radiation on the forest fuel layer.

2.4.2. Radiation released

The characterization of the heater was carried out to establish the incident radiative heat flux ($\dot{q}''_{inc}$) on the forest fuel and also to estimate the emitted radiative heat flux ($\dot{q}''_{emit}$) from the heater element at different voltages. In order to determine the profile of $\dot{q}''_{inc}$ a Medtherm Schmidt-Boelter radiometer with sapphire window was used together with the linear motor stage to scan and measure the incident radiation on the surface of the wildland fuel. On the other hand, considering that only a fraction of the emitted radiative heat flux is intercepted by the surface of the forest fuel layer, it is possible to obtain $\dot{q}''_{emit}$, using the view factor concept, $\dot{q}''_{emit} = \dot{q}''_{inc}/A_h F_{h\to i}$, where A_h is the area of the heater and $F_{h\to i}$ the fraction of the radiation leaving surface of the heater that is intercepted by surface of wildland fuel. An analytic expression is used for this factor Modest [27] considering the geometries indicated in Fig. 2.

The results obtained are presented in Fig. 3b. The heat fluxes observed at different positions are symmetrical independent of the voltage applied. For 250 V, the maximum incident radiative heat flux was about 30 kW/m^2, but on the ends it decreases up to 13.5 kW/m^2 correlated with the relative heater-radiometer position, in consequence, with the view factor.

Finally in Fig. 3c is presented the $\dot{q}''_{inc}$ in the left y-axis for different voltage applied. The $\dot{q}''_{elec} = VI/A_h$, $\dot{q}''_{bb} = \sigma T_h^4$ and $\dot{q}''_{emit}$ are plotted in the right y-axis. The concept $\dot{q}''_{elec}$ is the ratio of effective electric power (where V and I are the voltage and current, respectively) to the heater surface (A_h), $\dot{q}''_{bb}$ denotes the radiative heat flux emitted by the black body at mean temperature of the heater (T_h). As expected, $\dot{q}''_{bb}$ and $\dot{q}''_{emit}$ have the same trends observing small differences.

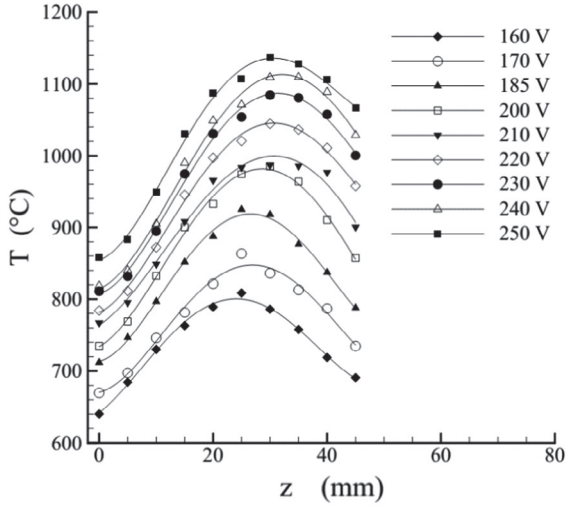

(a) Heater surface temperature at different voltages.

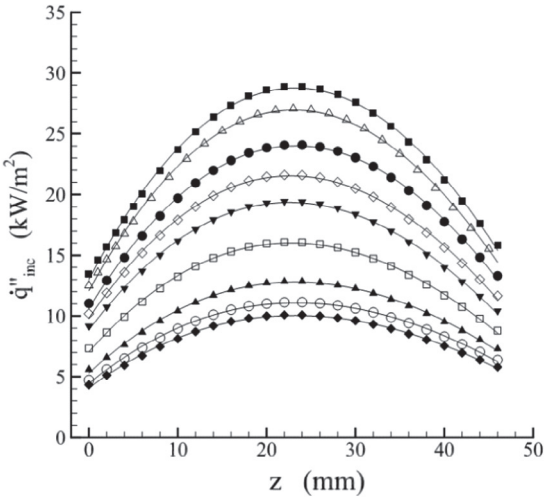

(b) Local incident radiative heat flux for different voltages measured at $r = r_i$.

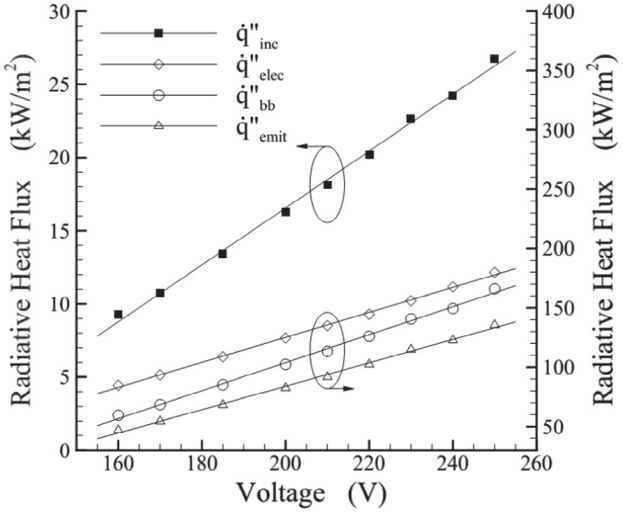

(c) Total heat and radiative heat flux released by the heater at different voltages.

Fig. 3. Heater element characterization.

2.5. Experimental procedure

Spontaneous ignition experiments were conducted in order to measure the time to ignition (t_{ig}), the time evolution of the radial temperatures (TC_j) and the mass (m) for different incident radiative heat fluxes on the forest fuel layer $\dot{q}''_{inc}$. After the preparation of the sample, following the procedure described above, the sample holder was placed on the analytical balance perfectly aligned with the heater axis of symmetry.

Prior to the time to ignition measurements, the steady state conditions of the heater element were assured. This was verified heating the element and controlling the radiant heat flux by a radiometer. The observed time to reach steady state was about 5 min for the highest voltage and the set of experiments presented in this work were carried out heating the element at the desire voltage or $\dot{q}''_{inc}$ for at least 10 min. Once the heater is ready the element was placed inside the forest fuel litter (see Fig. 2) using the linear motor and the measurements of time to ignition, current, voltage, mass loss and temperature were initiated and analyzed in real-time.

When the ignition occurred, the heater had to be quickly removed to avoid any damage from the flame. The sensors were still working and the measurements were stopped when no more visual changes were detected, otherwise if ignition did not take place, the measurements were stopped after 60 min. An experiment is defined by the $\dot{q}''_{inc}$ on the wildland surface and the volume fraction of the forest fuel sample. Each experiment was repeated at least 12 times ensuring the repeatability and the number of tests was increased close the critical heat flux for ignition where larger deviations were normally found.

3. Results

3.1. Ignition time

The ignition time behavior of the pine needles layer was characterized for the different parameters of this study following the methodology indicated above. In this study the ignition time was detected by visual recognition of the flame appearance, nevertheless, for the tested radiative heat fluxes some pine needles closer to heater exhibited glowing ignition. It was observed before flaming ignition and it is consistent with the study performed by Boonmee et al. [28]. Another method could be used to validate the ignition time. As shown in Fig. 4, for an incident radiative heat flux of $\dot{q}''_{inc}$=10.7 kW/m^2 and for different forest fuel arrangements, a drastic modification on the time evolution of mass loss ($\eta = 1-m/m_0$) and temperature (specially for TC_1) is observed at ignition. In both cases the ignition time is notably detected by mass loss or temperature and this methodology was used systematically to determine the spontaneous ignition time.

3.2. Critical heat flux

For each forest fuel layer sample considered, with fuel volume fractions of α=0.05 and α=0.08, experiments were carried out for different $\dot{q}''_{inc}$. The experimental campaign started from 26.7 kW/m^2, decreasing systematically by step of 2 kW/m^2 (10 V in the power supply) until the critical heat flux ($\dot{q}''_{inc,cri}$) was reached, when no ignition was observed after 60 min of exposition. The variation in the $\dot{q}''_{inc}$ was evaluated following the characterization presented in Fig. 3c. Once the eventual $\dot{q}''_{inc,cri}$ was reached the procedure proposed by Mindykowsky et al. [21] was implemented in order to determine its value. Basically, in this experiment the critical heat flux was defined as the minimum external heat radiant flux for spontaneous ignition. This value is somewhere between $\dot{q}''_{min,ig}$ and $\dot{q}''_{no,ig}$, denoting, respectively, the lowest incident heat flux at which ignition was observed and the highest incident heat flux at which ignition did not occur. The bounds of the critical heat fluxes were then refined by dichotomy obtaining a resolution of 0.5 kW/m^2. To validate $\dot{q}''_{inc,cri}$ experiments were allowed to continue after 120 min, until obvious changes in forest fuel layer appearance were no longer apparent. It is important to note that the number of test was increased near the critical heat flux for ignition where normally larger deviations were observed.

The results obtained for spontaneous ignition time are presented in Fig. 5a, where a slight difference in the critical heat flux is shown between curves for different volume fraction. For α=0.08 and α=0.05 the critical heat fluxes were 7.5 kW/m^2 and 10.4 kW/m^2, respectively. For lower heat fluxes no ignition was detected. The difference detected may be explained considering the forest fuel mass available for larger volume fractions. The mass of pyrolysis gases generated for larger α at the same $\dot{q}''_{inc}$ induces naturally a shorter spontaneous ignition time. This was observed in for the each experiments carried out. Same trends has been detected for piloted ignition of forest fuel layers [21]. Another important result is presented in Fig. 5b where the inverse of time to ignition was plotted [29]. For both forest fuel layer volume fractions is possible to deduce quasi-linear behavior. Again equivalent behaviors were obtained for forest fuel litters, in piloted and spontaneous ignition, when the pine needles are considered under the thermally thin approximation [21,30,31].

In this study the uncertainties were estimated by taking into account both of the statistical errors relative to the repeatability (u_a) and the instrument errors (u_b). As expected, the statistical errors, computed using the experimental standard deviation (s), were found to be larger. The only significant instrument error was associated to the radiometer (less than 3%). Then, statistical errors were calculated from the relationship $u_a = s/\sqrt{n}$, where the sample is n -size [32]. Finally, the combined uncertainty may be expressed as $u = \sqrt{u_a^2 + u_b^2}$.

3.3. Mass loss rate (MLR) before ignition

The large resolution obtained during the mass loss measurements allowed to detect with reliability small changes in the mass of pine needles, particularly in the pyrolysis process. Defining mass loss as $\eta = 1-m/m_0$ and the mass loss rate (MLR) as $d\eta/dt$ was possible to plot the evolutions presented in Fig. 6a and b, respectively. Both evolutions are possible to observe during the pyrolysis process, particularly before ignition for α=0.08 at different incident radiative heat fluxes, from the critical flux 7.5 kW/m^2 until the maximum flux applied of 26.7 kW/m^2. As expected, $\dot{q}''_{inc}$ has an important effect in η. Larger $\dot{q}''_{inc}$ induced monotonically large mass loss rate and shorter time to ignition.

Clearly the gradient of mass loss has a direct relation with the incident heat flux. In Fig. 6b has been plotted $d\eta/dt$ in order to compare the gradient of the mass loss at different volume fraction for fixed $\dot{q}''_{inc}$ of 18.1 kW/m^2. Once the ignition took place, the slope of η changed drastically and the mass loss increased significantly. Finally, in Fig. 6c is

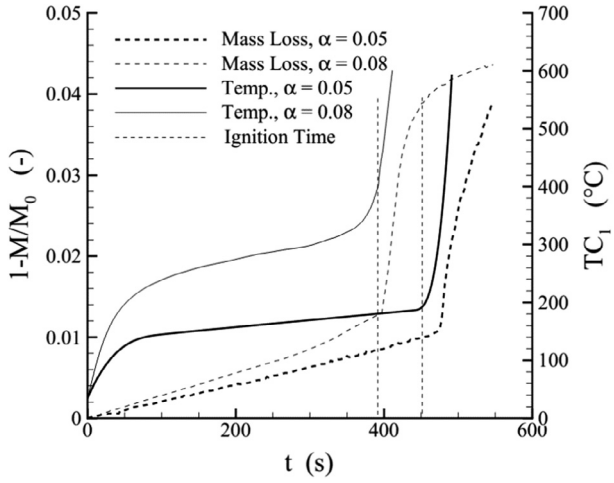

Fig. 4. Mass loss and temperature time evolution for $\dot{q}''_{inc}$=10.7 kW/m^2.

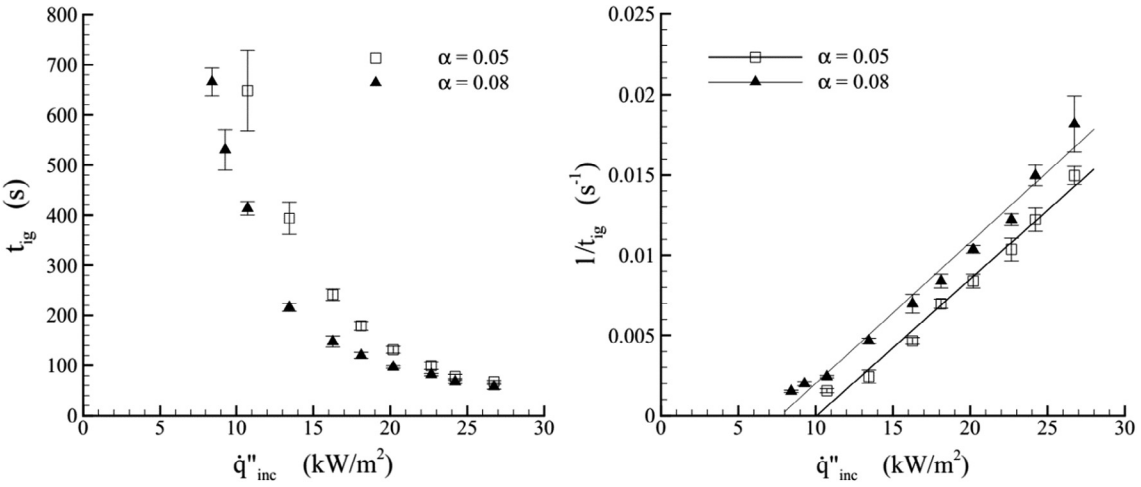

Fig. 5. Time to ignition at different incident radiative heat fluxes and for different volume fractions.

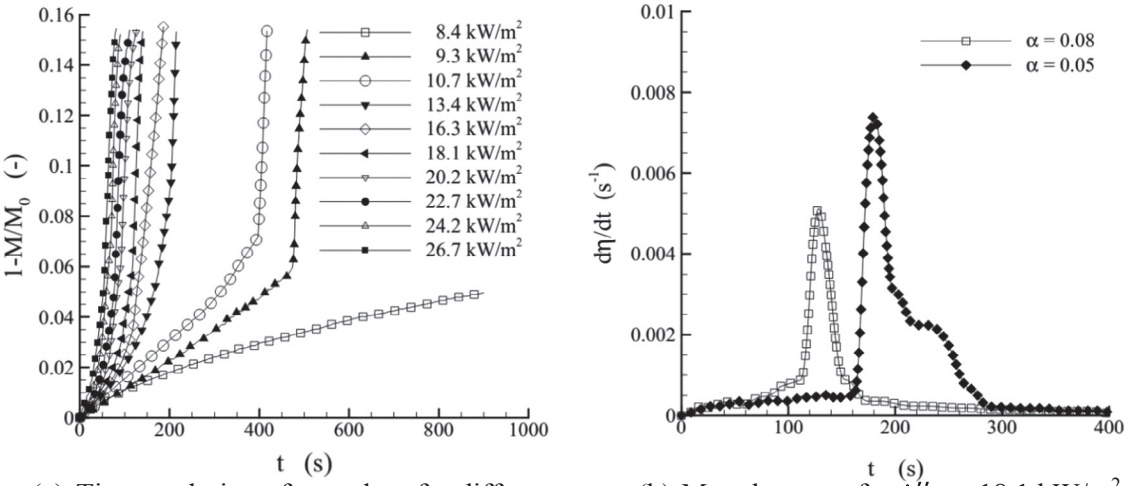

(a) Time evolution of mass loss for different $\dot{q}''_{inc}$ and for $\alpha = 0.08$.

(b) Mass loss rate for $\dot{q}''_{inc}$ = 18.1 kW/m^2.

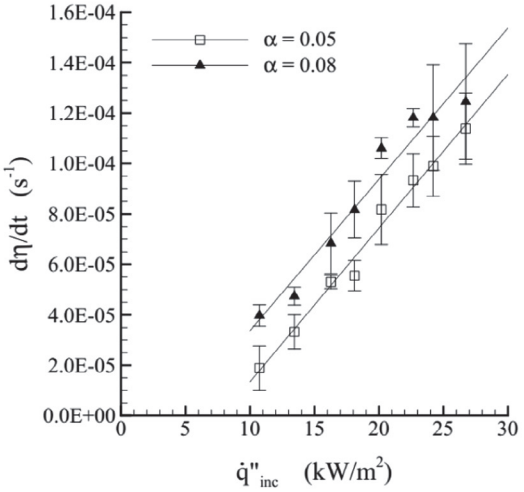

(c) Mass loss rate at different incident radiative heat fluxes.

Fig. 6. Time evolution of the mass loss before ignition at two volume fractions.

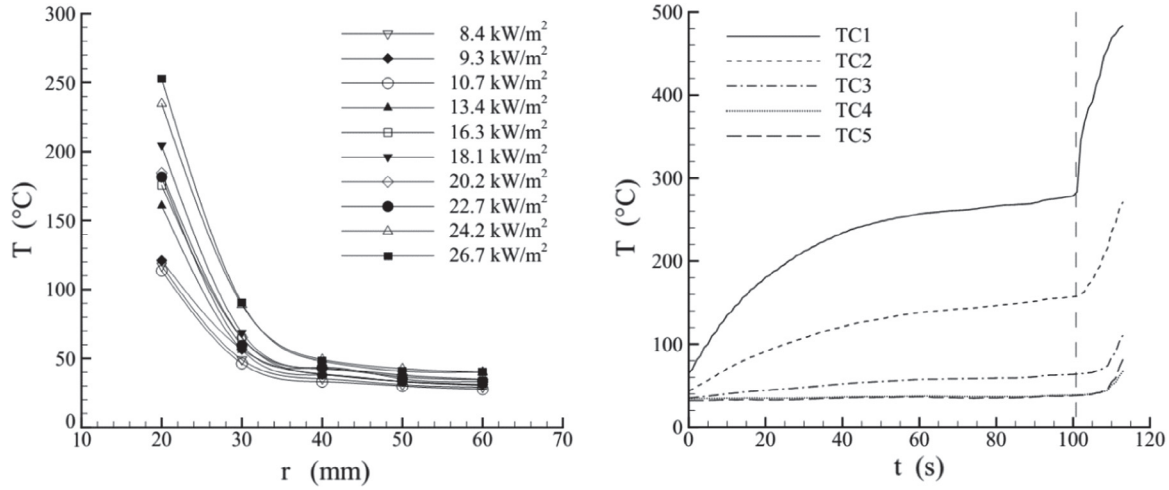

(a) Time evolution of radial temepratures at $\dot{q}''_{inc} = 20.2\ \mathrm{kW/m^2}$ and $\alpha = 0.05$.

(b) Temperature along r-axis at different $\dot{q}''_{inc}$ and for $\alpha = 0.08$.

Fig. 7. Time and spatial evolution of forest fuel layer temperature before ignition.

represented the mean MLR of the pyrolysis process before the ignition at different heat fluxes. The mean was evaluated as $(m_0-m_{t_{ig}})/t_{ig}$ for both α. As shown, MLR exhibits a quasi-linear behavior, similar relationship is found in the literature for piloted ignition considering MLR at the ignition time [33,34].

3.4. Forest fuel layer temperature

As presented in the experimental methodology five thermocouples (TC_j) were arranged along the radial axis (see Fig. 2) of forest fuel layer in order to study the time evolution of the temperatures. TC_1 was placed closest to heater element meanwhile TC_5 was positioned far from the heater axis. A typical result obtained for the five thermocouples are presented in Fig. 7a for a $\dot{q}''_{inc} = 20.2\ \mathrm{kW/m^2}$ and for α=0.05.

The two thermocouples closer to heater axis evidence a large effect and the penetration of radiant heat flux is then largely affected, generating slight modifications in the last two thermocouples. Clearly a drastic change was observed when the ignition took place. After the ignition the heat flux is larger and the five thermocouples are affected. The behavior is completely different for the no ignition tests, in general, the increasing of temperature is small with almost constant evolution.

Another interesting result is to study the radial temperature evolution inside the forest fuel layer for different heat fluxes. Fig. 7b presents the local radial temperatures profiles for α=0.08 and at a fixed time of 26 s. This time was chosen as the shorter time observed to reach the spontaneous ignition. As expected, temperature decreases monotonically with $\dot{q}''_{inc}$ independent of the local radial position inside the forest fuel layer.

4. Conclusions

An experimental study concerning the spontaneous ignition of a forest fuel layer by idealized firebrands was developed in a bench scale apparatus specifically designed to understand the relationship between the incident radiative heat flux and time to ignition. In this study the chosen firebrand was a cylindrical heater element with the geometry comprised in the range of common embers generated in real fires. Two fuel loads of Radiata Pine needles, with volume fractions of 0.05 and 0.08 were exposed at variable radiative heat flux, previously calibrated, under controlled conditions. A quasi-linear behavior between the inverse of time to ignition and incident radiative heat flux was obtained from the results as for thermally thin solid fuels. A dichotomy procedure was applied in order to estimate the critical heat fluxes to reach spontaneous ignition obtaining 7.5 $\mathrm{kW/m^2}$ and 10.4 $\mathrm{kW/m^2}$ for α=0.08 and α=0.05, respectively. From the experimental results, it is possible to deduce that time for spontaneous ignition decreases as the volume fraction increases. Also the uncertainties were estimated in ignition time considering mainly the statistical contribution. Mass loss and mass loss rate were measured and a linear behavior between mass loss rate and incident radiate heat flux was found, where a larger volume fraction leads to larger mass loss during the pyrolysis process. Local temperatures inside the forest fuel litter were also measured. Both mass loss rate and local temperature demonstrated that are a useful and objective way to determine the time to ignition, basically by the drastic changes exhibited once the ignition took place. Another interesting result involves the effect of the heat flux on the local temperatures. As expected, the local temperatures increase with the incident heat flux, independently of the thermocouple position. A thermal model is needed for an equivalent homogeneous medium and would be developed in the near future in order to improve the understanding of experimental evidence and to be extended to other fuel properties.

Acknowledgments

This work was partially supported by DGIIP-UTFSM Chile through the PIIC initiative.

References

[1] P. Reszka, A. Fuentes, The great valparaiso fire and fire safety management in Chile, Fire Technol. 51 (2015) 753–758.
[2] V. Babrauskas, Ignition Handbook, Fire Science Publishers, Washington, 2003.
[3] B. Porterie, N. Zekri, J.P. Clerc, J.C. Loraud, Modeling forest fire spread and spotting process with small world networks, Combust. Flame 149 (2007) 63–78.
[4] E. Koo, P. Pagni, D. Weise, J. Woycheese, Firebrands and spotting ignition in large-scale fires, Int. J. Wildland Fire 19 (2010) 818–843.
[5] A. Alexandridis, L. Russo, D. Vakalis, G. Bafas, S. Siettos, Wildland fire spread modelling using cellular automata: evolution in large-scalespatially heterogeneous environments under fire suppression tactics, Int. J. Wildland Fire 20 (2011) 633–647.
[6] F.A. Albini, Spot Fire Distance from Burning Trees: A Predictive Model, USDA Forest Service Intermountain Forest and Range Experiment Station, General Technical Report INT-56 (Odgen, UT.).
[7] C.S. Tarifa, P.P. Del Notario, F.G. Moreno, On the flight paths and lifetimes of burning particles of wood, Proc. Combust. Inst. 10 (1965) 1021–1037.
[8] S.D. Tse, A.C. Fernandez-Pello, On the flight paths of metal particles and embers generated by power lines in high winds and their potential to initiate wildfires, Fire Safety. 30 (1998) 333–356.
[9] J.P. Woychesse, Brand Lofting and Propagation for Large-Scale Fires, Ph.D. Thesis,

University of California, Berkeley, 2000.
[10] W.H. Blackmarr, Moisture Content Influences Ignitability of Slash Pine Litter, USDA Forest Service, Southeastern Forest Experiment Station, Research Note RN-SE-173 (Asheville, NC).
[11] A.D. Ferreira, Ignição de combustíveis finos por fósforos, Actas das Jornadas Científicas sobre Incêndios Florestais, University of Coimbra, Coimbra, Portugal, 1988.
[12] S.L. Manzello, A. Maranghides, W.E. Mell, T.G. Cleary, J.C. Yang, Firebrand production from burning vegetation, in: V International Conference on Forest Fire Research, Figueira da Foz, Portugal, 2006.
[13] S.L. Manzello, T.G. Cleary, J.R. Shields, J.C. Yang, On the ignition of fuel beds by firebrands, Fire Mater. 30 (2006) 77–87.
[14] P.F. Ellis, The Aerodynamic and Combustion Characteristics of Eucalypt Bark — A Firebrand Study, Ph.D. dissertation, Australian National University, Canberra, 2000.
[15] W.W. Hargrove, R.H. Gardner, M.G. Turner, W.H. Romme, D.G. Despain, Simulating fire patterns in heterogeneous landscapes, Ecol. Model. 135 (2000) 243–263.
[16] A. Ganteaume, C. Lampin-Maillet, M. Guijarro, C. Hernando, M. Jappiot, T. Fonturbel, P. Perez-Gorostiaga, J. Vega, Spot fires: fuel bed flammability and capability of firebrands to ignite fuel beds, Int. J. Wildland Fire 18 (2009) 951–969.
[17] N. Sardoy, J.L. Consalvi, A. Kaiss, A.C. Fernandez-Pello, B. Porterie, Numerical study of ground-level distribution of firebrands generated by line fires, Combust. Flame 154 (2008) 478–488.
[18] S.L. Manzello, A. Maranghides, J.R. Shields, W.E. Mell, Y. Hayashi, D. Nii, Mass and size distribution of firebrands generated from burning Korean pine (Pinus koraiensis) trees, Fire Mater. 33 (2009) 21–31.
[19] R.H. White, D.R. Weise, D. De Mars, M. Bishop, Flammability of Christmas Trees and Other Vegetation, in: Proceedings of the 24th International Conference on Fire Safety, Products Safety Corporation, Ohio, 1997.
[20] A.P. Dimitrakopoulos, K.K. Papaioannou, Flamability assessment of Mediterranean forest fuels, Fire Technol. 37 (2001) 143–152.
[21] P. Mindykowski, A. Fuentes, J.L. Consalvi, B. Porterie, Piloted ignition of wildland fuels, Fire Saf. J. 46 (2010) 34–40.
[22] A.V. Filippov, Flamability assessment of Mediterranean forest fuels, Fire Technol. 37 (2001) 143–152.
[23] L. Trabaud, Inflammabilité et Combustibilité des Principales Espèces des Garrigues de la Region Méditerranéenne, Œcol Plat. 11 (1976) 171–177.
[24] V. Tihay, P.A. Santoni, T. Barboni, L. Leonlli, Autoignition of dead shrub twigs: influence of diameter on ignition, Fire Technol. 52 (2016) 897–929.
[25] J.L. Urban, C.D. Zak, J. Song, C. Fernandez-Pello, Smoldering spot ignition of natural fuels by a hot metal particle, Proc. Combust. Inst. 36 (2017) 3211–3218.
[26] V. Tihay, A. Simeoni, P.A. Santoni, L. Rossi, J.P. Garo, J.P. Vantelon, Experimental study of laminar flames obtained by the homogenization of three forest fuels, Int. J. Therm. Sci. 48 (2009) 488–501.
[27] F.M. Modest, Radiative Heat Transfer, Academic Press, Elsevier, Oxford, 2013.
[28] N. Boonmee, J.G. Quintiere, Glowing and flaming autoignition, Proc. Combust. Inst. 29 (2002) 289–296.
[29] E. Mikkola, I.S. Wichman, On the thermal ignition of combustible materials, Fire Mater. 14 (1989) 87–96.
[30] S. McAllister, M. Finney, Autoignition of wood under combined convective and radiative heating, Proc. Combust. Inst. 36 (2017) 3073–3080.
[31] S. McAllister, I. Grenfell, A. Hadlow, W. Jolly, M. Finney, J. Cohen, Piloted ignition of live forest fuels, Fire Saf. J. 51 (2012) 133–142.
[32] J.R. Taylor, Error Analysis, The Study of Uncertainties in Physical Measurements, University Science Books, California, 1997.
[33] S. McAllister, M. Finney, J. Cohen, Critical mass flux for flaming ignition of wood as a function of external radiant heat flux and moisture content, in: 7th US National Technical Meeting of the Combustion Institute, Atlanta, 2011.
[34] S. McAllister, Critical mass flux for flaming ignition of wet wood, Fire Safety 61 (2013) 200–206.